Geophys. J. Int. (2008) **174,** 585–592 doi: 10.1111/j.1365-246X.2008.03797.x

Stable inversions for complete moment tensors

Sarah E. Minson[1] and Douglas S. Dreger[2]

[1] *Seismological Laboratory, California Institute of Technology, Pasadena,* CA 91125*, USA.*
E-mail: minson@gps.caltech.edu
[2] *Department of Earth and Planetary Science, University of California, Berkeley,* CA 94720*, USA*

Accepted 2008 March 16. Received 2008 March 16; in original form 2008 January 12

SUMMARY

The seismic moment tensors for certain types of sources, such as volcanic earthquakes and nuclear explosions are expected to contain an isotropic component. Some earlier efforts to calculate the isotropic component of these sources are flawed due to an error in the method of Jost & Herrmann. We corrected the method after Herrmann & Hutchensen and found great improvement in the recovery of non-double-couple moment tensors that include an isotropic component. Tests with synthetic data demonstrate the stability of the corrected linear inversion method, and we recalculate the moment tensor solutions reported in Dreger *et al.* for Long Valley caldera events and Dreger & Woods for Nevada Test Site nuclear explosions. We confirm the findings of Dreger *et al.* that the Long Valley volcanic sources contain large statistically significant isotropic components. The nuclear explosions have strikingly anomalous source mechanisms, which contain very large isotropic components, making it evident that these events are not tectonic in origin. This indicates that moment tensor inversions could be an important tool for nuclear monitoring.

Keywords: Inverse theory; Earthquake source observations; Seismic monitoring and test-ban treaty verification; Volcano seismology; Computational seismology; Theoretical seismology.

1 INTRODUCTION

Earthquake source mechanisms are routinely determined through moment tensor inversions. This process requires that synthetic seismograms be represented as the linear combination of fundamental Green's functions, where the weights on these Green's functions are the individual moment tensor elements. An analytical representation of this system for a general moment tensor was derived in Jost & Herrmann (1989) (appendix A), based on the work of Langston (1981) for a deviatoric (zero trace) moment tensor (Method 1). However, an error in the Jost & Herrmann (1989) derivation precludes their moment tensor inversion scheme from correctly recovering source mechanisms which include isotropic components, although it is accurate for analysing deviatoric sources. In this paper, we present a correction to their inversion scheme after Herrmann & Hutchensen (1993) (Method 2). Method 2 can accurately recover moment tensors for both deviatoric and non-deviatoric sources. Tests of this method using synthetic data show that it works well, and we have used the new inversion scheme to determine moment tensors for several real volcanic and nuclear explosion sources.

2 METHODOLOGY

Analytical solutions for surface displacement have been derived for a double-couple source (Helmberger 1983), a deviatoric source (Langston 1981) and for a general moment tensor (Jost & Herrmann 1989). A deviatoric point source can be represented by using Green's functions for three fundamental faults: a vertical strike-slip fault; a vertical dip-slip fault and a dip-slip fault with a dip of 45° (Langston 1981). However, for a complete moment tensor, $\boldsymbol{M}$, we must also include the explosion Green's functions, so that

$$\begin{aligned} u_Z &= A_1 \cdot ZSS + A_2 \cdot ZDS + A_3 \cdot ZDD + M_{\text{iso}} \cdot ZEP, \\ u_R &= A_1 \cdot RSS + A_2 \cdot RDS + A_3 \cdot RDD + M_{\text{iso}} \cdot REP, \\ u_T &= A_4 \cdot TSS + A_5 \cdot TDS, \end{aligned} \tag{1}$$

where u is the surface displacement, *SS* is the vertical strike-slip Green's function, *DS* is the vertical dip-slip Green's function, *DD* is the 45° dip-slip Green's function and *EP* is the explosion Green's function. *Z*, *R* and *T* refer to the vertical, radial and tangential components, respectively, and

$$M_{\text{iso}} = \frac{\text{tr}(\mathbf{M})}{3}. \tag{2}$$

It is in the calculation of the A_i coefficients that the two methods diverge.

2.1 Method 1 (Jost & Herrmann 1989)

Method 1 wrongly uses the A_i coefficients for a deviatoric source,

$$\begin{aligned} A_1 &= \frac{1}{2}(M_{xx} - M_{yy})\cos(2az) + M_{xy}\sin(2az), \\ A_2 &= M_{xz}\cos(az) + M_{yz}\sin(az), \\ A_3 &= -\frac{1}{2}(M_{xx} + M_{yy}), \end{aligned}$$

$$A_4 = \frac{1}{2}(M_{xx} - M_{yy})\sin(2az) - M_{xy}\cos(2az),$$
$$A_5 = -M_{yz}\cos(az) + M_{xz}\sin(az), \quad (3)$$

where M_{ij} are the elements of the moment tensor and az is the source–receiver azimuth. It should be noted that since the seismic moment tensor is symmetric, it has only six independent elements.

Eq. (3) is the same as eq. A5.3 in Jost & Herrmann (1989), which in turn is eq. 3 in Langston (1981) transformed into a coordinate system where z is positive up and the positive tangential direction is measured clockwise from north.

2.2 Method 2 (Herrmann & Hutchensen 1993; this paper)

Since any tensor can be described as the sum of deviatoric and isotropic tensors, we describe each synthetic seismogram as the sum of a synthetic seismogram with a deviatoric source and one with an isotropic source. For the deviatoric synthetic seismograms, we retain the Langston (1981) formulae (eq. 3). However, we replace the A_i coefficients with $A_i{}^*$, which are the A_i coefficients calculated from the elements of the deviatoric part of the full moment tensor, $M_{ij}{}^*$ where,

$$M^*_{xx} = M_{xx} - \frac{M_{xx} + M_{yy} + M_{zz}}{3},$$
$$M^*_{yy} = M_{yy} - \frac{M_{xx} + M_{yy} + M_{zz}}{3},$$
$$M^*_{zz} = M_{zz} - \frac{M_{xx} + M_{yy} + M_{zz}}{3},$$
$$M^*_{xy} = M_{xy},$$
$$M^*_{xz} = M_{xz},$$
$$M^*_{yz} = M_{yz}. \quad (4)$$

Substituting M^*_{ij} into eq. (3), we obtain

$$A^*_1 = A_1,$$
$$A^*_2 = A_2,$$
$$A^*_3 = -\frac{1}{6}(M_{xx} + M_{yy} - 2M_{zz}),$$
$$A^*_4 = A_4,$$
$$A^*_5 = A_5. \quad (5)$$

Note that for a deviatoric moment tensor for which eq. (3) must hold, eq. (5) is identical to eq. (3).

Substituting eq. (5) into eq. (1) and rearranging, we find

$$u_z = M_{xx}\left[\frac{ZSS}{2}\cos(2az) - \frac{ZDD}{6} + \frac{ZEP}{3}\right] + M_{yy}\left[-\frac{ZSS}{2}\cos(2az) - \frac{ZDD}{6} + \frac{ZEP}{3}\right] + M_{zz}\left[\frac{ZDD}{3} + \frac{ZEP}{3}\right] + M_{xy}[ZSS\sin(2az)] + M_{xz}[ZDS\cos(az)] + M_{yz}[ZDS\sin(az)], \quad (6)$$

$$u_r = M_{xx}\left[\frac{RSS}{2}\cos(2az) - \frac{RDD}{6} + \frac{REP}{3}\right] + M_{yy}\left[-\frac{RSS}{2}\cos(2az) - \frac{RDD}{6} + \frac{REP}{3}\right] + M_{zz}\left[\frac{RDD}{3} + \frac{REP}{3}\right] + M_{xy}[RSS\sin(2az)] + M_{xz}[RDS\cos(az)] + M_{yz}[RDS\sin(az)], \quad (7)$$

$$u_t = M_{xx}\left[\frac{TSS}{2}\sin(2az)\right] + M_{yy}\left[-\frac{TSS}{2}\sin(2az)\right] + M_{xy}[-TSS\cos(2az)] + M_{xz}[TDS\sin(az)] + M_{yz}[-TDS\cos(az)]. \quad (8)$$

Note that these equations differ from eqs 5.4–5.6 in Jost & Herrmann (1989). However, this is the same result as was obtained in Herrmann & Hutchensen (1993).

2.3 Comparison

To illustrate why Method 2 is correct and Method 1 is flawed, consider a purely isotropic source,

$$M_{xx} = M_{yy} = M_{zz} = M_{\rm iso},$$
$$M_{xy} = M_{xz} = M_{yz} = 0. \quad (9)$$

Intuitively, the synthetic seismograms for this source should be,

$$u_z = M_{\rm iso}ZEP,$$
$$u_r = M_{\rm iso}REP,$$
$$u_t = 0. \quad (10)$$

This is exactly the solution obtained by eqs (6)–(8). However, the Method 1 (Jost & Herrmann 1989) equations produce

$$u_z = M_{\rm iso}[ZEP - ZDD],$$
$$u_r = M_{\rm iso}[REP - RDD],$$
$$u_t = 0. \quad (11)$$

Thus, if a non-deviatoric moment tensor is used in the Method 1 equations, then the isotropic component is not only used to weight the isotropic Green's functions *ZEP* and *REP* but also incorrectly weights the *ZDD* and *RDD* deviatoric Green's functions, and thus full moment tensor inversions implementing the Method 1 equations are incapable of accurately recovering an isotropic component. The Method 2 inversion system presented in this paper (from Herrmann & Hutchensen 1993) eliminates that problem.

3 RESULTS

3.1 Tests with synthetic data

To test the efficacy of Method 2, we inverted synthetic data for many different source mechanisms. We used Green's functions calculated by frequency–wavenumber integration (Saikia 1994) for a

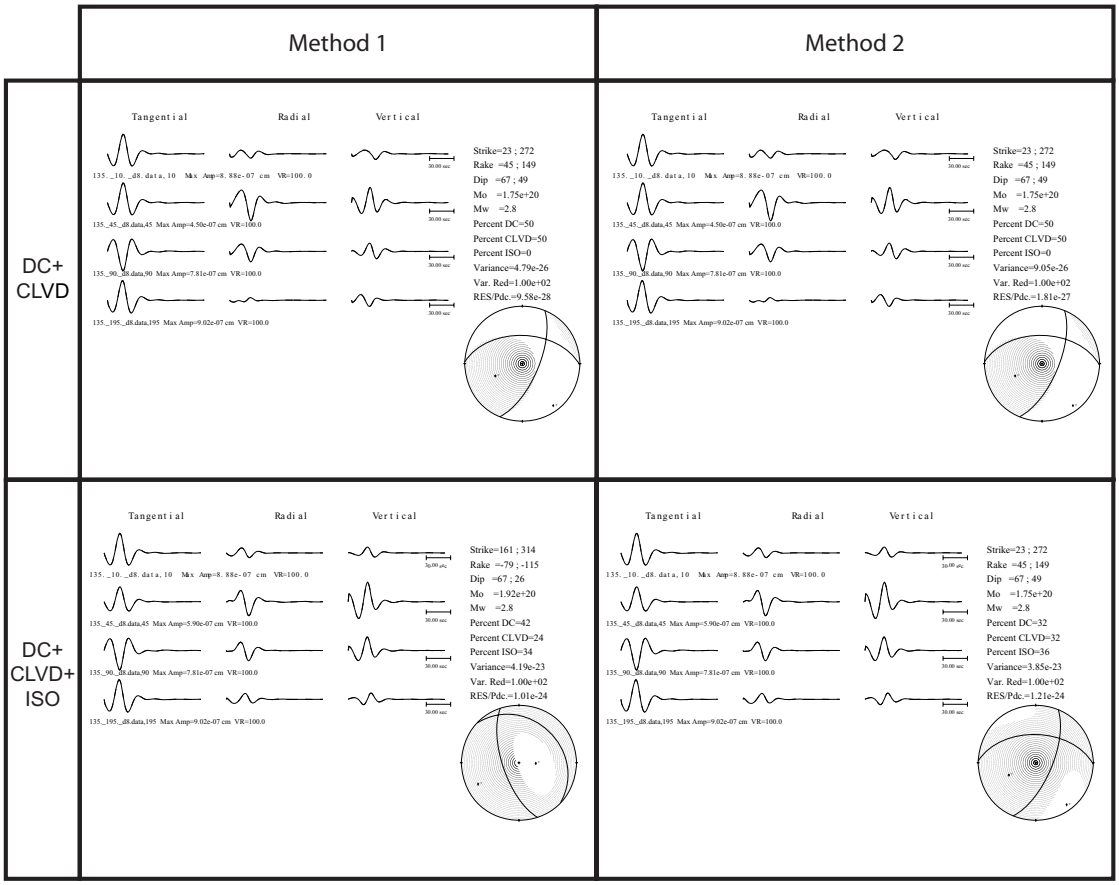

Figure 1. Comparison of full moment tensor inversions of synthetic data using the equations from Jost & Herrmann (1989) (Method 1) with the ones introduced in this paper (Method 2). (Top) inversions of a deviatoric mechanism comprised of a double-couple component (strike 23°, dip 67°, rake 45°) and a compensated linear vector dipole (CLVD) component, with the same moment and principal axes as the double-couple. The stations are located at a distance of 135 km and the source is at a depth of 8 km. Method 1 and Method 2 result in identical mechanisms. (Bottom) inversions of a non-deviatoric source. The deviatoric part of the input source mechanism is the same as that in (Top). Method 1 results in a completely different mechanism. In contrast, the method introduced in this paper (Method 2) recovers the original deviatoric mechanism as well as the added isotropic component.

1-D velocity structure, and bandpass filtered these Green's functions between 20 and 50 s period with an acausal Butterworth filter. The synthetic data were constructed using the same filtered Green's functions and inverted using a linear time domain moment tensor inversion (Pasyanos *et al.* 1996; Fukuyama & Dreger 2000).

Fig. 1 is a sample comparison of inversions of deviatoric and non-deviatoric synthetic data. For deviatoric source mechanisms, both inversion methods result in the same mechanisms, which is expected since Method 1 is accurate for deviatoric sources. When we add an isotropic component to those same synthetic data, Method 1 is not able to recover the elements of the moment tensor. In contrast, Method 2 returns the actual source mechanism.

3.2 Application to real data

We applied Method 2 to actual data from several real non-double-couple sources: three Nevada Test Site (NTS) nuclear explosions (BEXAR, MONTELLO and JUNCTION) in 1991 and 1992; the 1997 Mammoth earthquake swarm in the Long Valley caldera (LV1–LV6) and the earthquake swarm associated with the Miyakejima, Japan volcanic eruption in 2000 (MIYVOL) (see Table 1). We also investigated several tectonic earthquakes from the same three source regions (SKULL, LVTEC and MIYTEC) (Table 1). The NTS explosions were previously studied by Dreger & Woods (2002) using Method 1. Dreger & Woods (2002) found that the NTS explosions had very anomalous mechanisms, which could be used to help distinguish them from naturally occurring earthquakes. The full moment tensor results had large isotropic components, but they were not statistically significant and were found to suffer from a trade-off with a vertically oriented compensated linear vector dipole (CLVD) component (Knopoff & Randall 1970). The deviatoric inversions had large, predominantly vertically oriented CLVDs that were consistent with the nuclear explosion mechanisms reported in Patton (1988). This inability to recover the explosive nature of the source could be due to free-surface effects; and other studies have found that isotropic components of shallow events are difficult to constrain (e.g. Patton 1988; Dufumier & Rivera 1997). However, after repeating this study using Method 2, it appears that these events actually contain large isotropic components (Fig. 2, Table 2). Furthermore, sensitivity tests show that it is possible to resolve isotropic components of moment tensors for NTS explosions with source depths as small as 300 m (Ford *et al.* 2007). These new mechanisms clearly identify BEXAR, MONTELLO and JUNCTION as being principally explosive and non-tectonic in origin.

In addition to the NTS explosions, we studied volcanic earthquakes from the Long Valley caldera, California (LV1–LV6, Fig. 3, Table 3) and from Miyakejima, Japan (MIYVOL, Fig. 4,

Table 1. Hypocenter information.

Event name	Description	Origin time (UT)	Latitude	Longitude	M_L
SKULL	Tectonic earthquake	06/29/1992 10:14:20.1	36.638	−116.171	6.2
BEXAR	Nuclear explosion	04/04/1991 19:00:00.0	37.296	−116.313	5.6
MONTELLO	Nuclear explosion	04/16/1991 15:30:00.0	37.245	−116.442	5.4
JUNCTION	Nuclear explosion	03/29/1992 16:30:00.0	37.272	−116.360	5.5
LVTEC[a]	Tectonic earthquake	11/02/1997 08:51:53.9	37.846	−118.215	5.3[c]
LV1[a]	Volcanic earthquake	11/22/1997 12:06:56.0	37.635	−118.917	4.5
LV2[a]	Volcanic earthquake	11/22/1997 17:20:35.1	37.636	−118.936	4.8
LV3[a]	Volcanic earthquake	11/22/1997 18:10:59.4	37.634	−118.951	4.7
LV4[a]	Volcanic earthquake	11/30/1997 21:17:05.4	37.634	−118.946	4.8
LV5[a]	Volcanic earthquake	07/15/1998 04:53:19.3	37.564	−118.806	5.1
LV6[a]	Volcanic earthquake	05/15/1999 17:54:08.8	37.509	−118.831	4.7
MIYTEC[b]	Tectonic earthquake	07/30/2000 12:25:46.6	33.968	139.414	–
MIYVOL[b]	Volcanic earthquake	07/01/2000 07:01:56.3	34.187	−139.197	–

[a] Advanced National Seismic System (ANSS) composite catalogue
[b] Japan Meteorological Agency (JMA) catalogue
[c] M_c

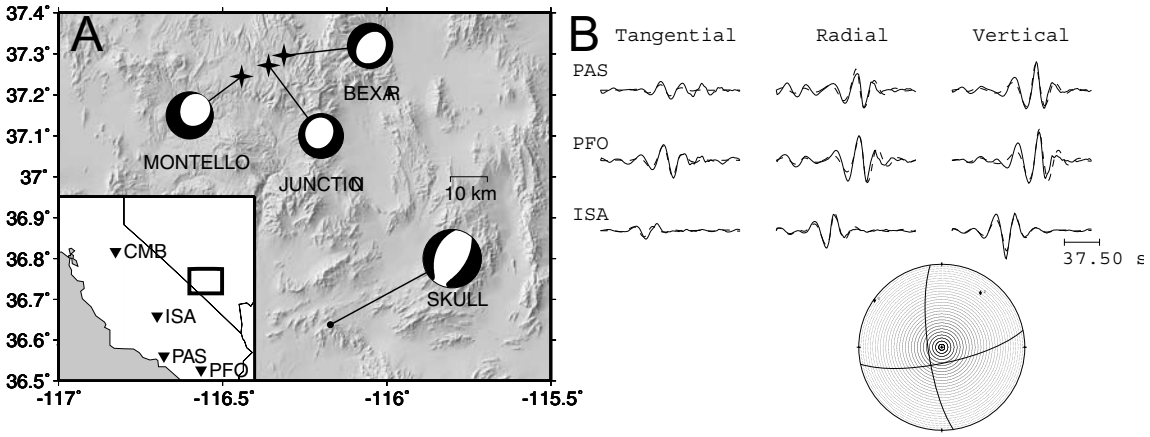

Figure 2. (a) Location map and station distribution used for inversion of NTS explosions and Little Skull Mountain earthquake. Focal mechanisms are based on deviatoric moment tensor inversions (Dreger & Woods 2002). (b) Focal mechanism and waveform fits from the new full moment tensor inversion for BEXAR (Table 1). Data are plotted with solid lines, synthetics with dashed lines. The new moment tensor inversion, which employs the corrected equations presented in this paper, reproduces the observed waveforms very well. The resulting focal mechanism clearly shows that the source was explosive.

Table 4). LV5 and LV6 are predominantly double-couple earthquakes, and thus the different inversion methods result in nearly identical mechanisms. Using Method 1, LV1, LV2 and LV4 appear to have mechanisms that are combinations of normal faulting, CLVD components and isotropic components. LV3 is similar but it has a strike-slip double-couple component. Using Method 2, these four Long Valley earthquakes behave very similarly to the NTS explosion mechanisms: the new mechanisms are comprised mostly of double-couple and isotropic (DC + ISO) components with a small CLVD component. This is consistent with other studies which found that regional data for events in the Long Valley caldera are best fit by DC + ISO mechanisms (Templeton & Dreger 2006).

The Miyakejima volcanic event seems somewhat different from the other events studied. The new mechanism is very complicated,

Table 2. Mechanisms for Little Skull Mountain earthquake and NTS explosions.

		T-axis			*I*-axis			*P*-axis		
	Event	Value	Trend	Plunge	Value	Trend	Plunge	Value	Trend	Plunge
Dreger & Woods (2002)	SKULL	278.80	116.96	8.89	−32.67	−151.36	10.61	−296.20	−12.21	76.09
	BEXAR	9.82	−54.88	0.11	7.61	−144.88	2.22	−4.40	37.98	87.77
	MONTELLO	13.50	−53.21	3.92	8.95	−143.95	10.67	−5.76	56.67	78.61
	JUNCTION	10.03	102.52	5.21	8.99	−167.42	0.68	−3.74	−70.05	84.74
This study	SKULL	294.40	116.85	8.17	−17.45	−151.85	9.01	−326.90	−14.73	77.79
	BEXAR	5.48	−55.16	1.45	4.48	−149.00	69.21	3.07	35.39	20.73
	MONTELLO	8.76	−70.66	35.92	6.70	163.73	38.79	1.24	45.01	30.88
	JUNCTION	7.21	107.25	62.40	4.20	−94.19	25.95	3.87	0.11	8.76

Note: Eigenvalues are given in 10^{15} N m. Orientations (trend and plunge) are given in degrees.

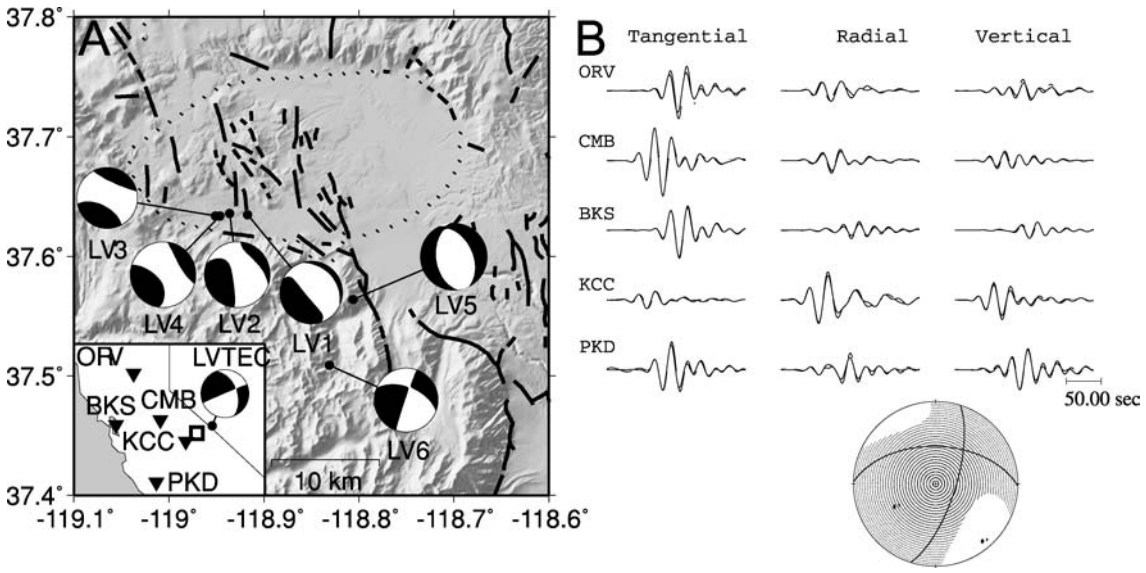

Figure 3. (a) Location map and station distribution used for inversion of Long Valley volcanic earthquakes. Focal mechanisms are based on deviatoric moment tensor inversions (Dreger *et al.* 2000). (b) Focal mechanism and waveform fits from the new full moment tensor inversion for LV2 (Table 1). Data are plotted with solid lines, synthetics with dashed lines. This mechanism, calculated with the corrected equations, is predominantly comprised of double-couple and isotropic components.

Table 3. Same as Table 2 for Long Valley earthquakes.

		T-axis			*I*-axis			*P*-axis		
	Event	Value	Trend	Plunge	Value	Trend	Plunge	Value	Trend	Plunge
Dreger *et al.* (2000)	LVTEC	92.70	−58.34	28.25	−4.38	68.34	48.03	−104.90	−165.08	28.19
	LV1	13.42	−131.07	22.92	3.80	−40.23	2	−6.38	54.49	66.99
	LV2	40.92	−122.48	16.98	5.48	−26.42	19.05	−9.20	108.71	64.02
	LV3	12.49	−154.69	10.34	0.28	−64.22	2.56	−3.23	39.53	79.34
	LV4	45.54	−124.75	9.91	8.81	143.99	7.14	−2.73	18.78	77.74
	LV5	34.25	−106.48	0.33	5.54	−16.43	9.70	−27.89	161.57	80.29
	LV6	13.65	−110.48	18.20	0.53	6.98	54.52	−10.09	148.89	29.29
This study	LVTEC	94.90	−59.32	25.03	−7.96	61.28	47.47	−103.50	−166.16	31.82
	LV1	12.58	−130.43	39.13	0.24	−34.50	7.24	−1.98	64.19	49.94
	LV2	38.49	−110.53	51.62	15.32	40.79	34.80	−7.99	140.89	14.16
	LV3	10.01	−154.51	23.56	2.45	21.17	66.38	−2.91	114.80	1.58
	LV4	38.88	−126.98	55.74	21.38	57.57	34.17	−8.64	−33.87	2.12
	LV5	30.29	−106.47	0.41	2.08	−16.36	14.75	−20.47	161.96	75.25
	LV6	12.81	−109.07	24.09	1.98	23.06	56.31	−10.70	150.49	22.06

and the CLVD component actually increases. This event is located along the NW trending earthquake swarm. This swarm is argued to be due to an inflating dyke related to the caldera collapse of Mount Oyama on Miyakejima (e.g. Nishimura *et al.* 2001; Furuya *et al.* 2003). The complex mechanism, including the isotropic component, indicates that MIYVOL has a fluid-controlled source process.

We also applied both methodologies to tectonic earthquakes from all three source regions to make sure that our non-double-couple components were not artefacts from path effects. These earthquakes are the SKULL earthquake which occurred near the NTS, LVTEC near Long Valley and MIYTEC near Miyakejima (Table 1). In all cases, both methodologies yielded double-couple mechanisms for the tectonic earthquakes, indicating that our inferred earthquake source mechanisms are not being contaminated by unmodelled Earth structure or biases due to the source–receiver geometries (Fig. 5).

4 DISCUSSION AND CONCLUSIONS

Inversions of synthetic data (Fig. 1) show that the corrected inversion, Method 2, is capable of accurately recovering both deviatoric source mechanisms and mechanisms containing isotropic components. With Method 2, we find that several volcanic earthquakes and nuclear explosions have mechanisms with larger isotropic components, smaller CLVD components and smaller total moments, than the mechanisms determined using the incorrect inversion scheme, Method 1 (Fig. 5, Table 5). Most of these mechanisms appear to be predominantly DC + ISO.

Method 2 is the correct full moment tensor inversion methodology, and the Method 2 mechanisms presented in this paper are meant to replace the solutions in Dreger *et al.* (2000) and Dreger & Woods (2002). Although the two full moment tensor inversion methodologies result in very different solutions, the solutions fit the data the same. Thus, the statistical analyses in Dreger *et al.* (2000) and Dreger & Woods (2002) are unchanged.

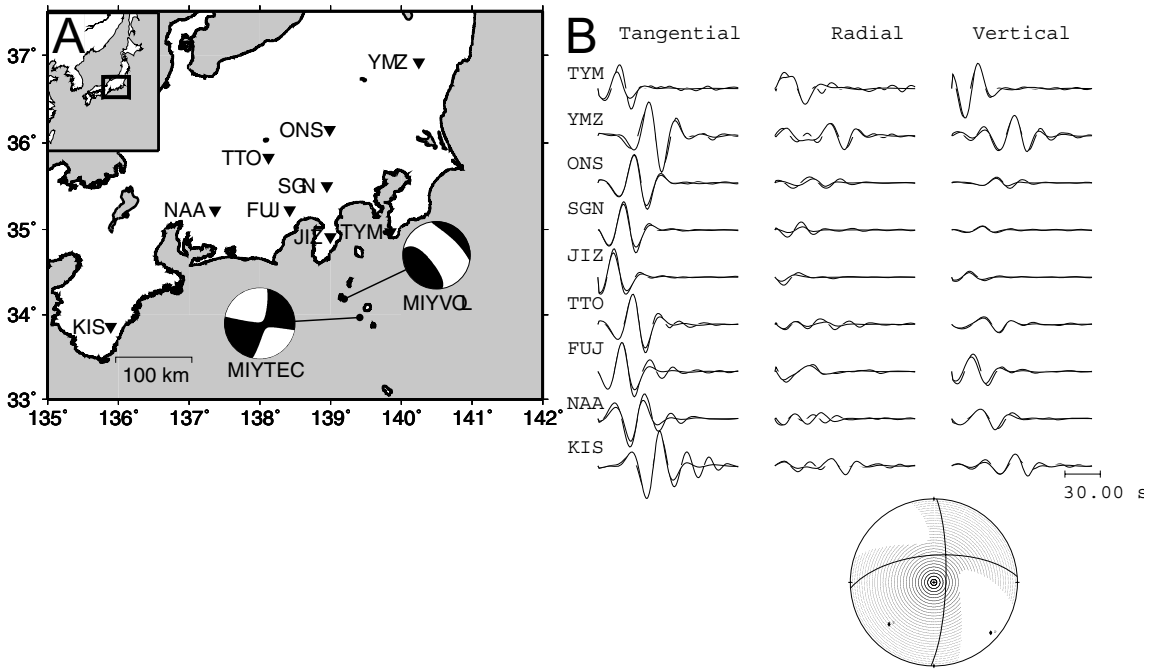

Figure 4. (a) Location map and station distribution used for inversion of a Miyakejima volcanic earthquake. Focal mechanism is based on a deviatoric moment tensor inversion. (b) Focal mechanism and waveform fits from the new full moment tensor inversion for MIYVOL (Table 1). Data are plotted with solid lines, synthetics with dashed lines. The new inversion scheme produces a complex mechanism containing double-couple and isotropic components as well as a large CLVD component.

Table 4. Same as Table 2 for Miyakejima earthquakes.

		T-axis			*I*-axis			*P*-axis		
	Event	Value	Trend	Plunge	Value	Trend	Plunge	Value	Trend	Plunge
Method 1	MIYTEC	5619	−123.7	4.82	−173.1	125.55	76.61	−3375	−32.63	12.47
	MIYVOL	2931	−133.73	15.10	111.1	−41.96	6.55	−1035	70.81	73.48
Method 2	MIYTEC	4951	−123.9	7.4	1125	102.4	79.36	−4006	−32.9	7.61
	MIYVOL	2508	−133.14	27.37	98.20	23.30	60.54	−599.7	131.60	10.05

One concern with full moment tensor inversions is that they can yield larger moments than a deviatoric moment tensor inversion for the same event. Such increases in moment can be caused by trade-offs between elements of the moment tensor and thus indicate that the full moment tensor solution may be invalid (Dreger & Woods 2002). However, for the non-tectonic earthquakes, Method 2 results in moments which are smaller than the moments from Method 1—the original incorrect full moment tensor inversion methodology (Table 5).

Woods *et al.* (1993) proposed using an M_L: M_0 differential measure as a regional discriminant for nuclear explosions. Method 1 inflated the apparent moment magnitude of the three NTS explosions. Method 2 decreases the moment magnitudes of these events, thereby increasing the $M_L - M_W$ differential, making it easier to distinguish these sources from normal earthquakes. Thus, it appears that moment tensor inversions could be a useful tool for nuclear monitoring.

Compared with the results from Method 1 (Dreger *et al.* 2000), the Method 2 source mechanisms for LV2, LV3 and LV4 have smaller CLVD components. These Method 2 moment tensors obtained by full moment tensor inversion are in agreement with the results obtained by Templeton & Dreger (2006) using a grid search technique. The double-couple components of LV2, LV3 and LV4 have an east–west striking steeply-dipping nodal plane, with a right-lateral sense of motion that is consistent with the trend of background seismicity in the south moat of the caldera, as well as focal mechanisms of smaller events. These source mechanisms are consistent with shear-faulting on pre-existing planes, following injection of high pressure fluid or gas as Julian & Sipkin (1985) suggested for the 1980 Long Valley swarm.

We also used Method 2 to recompute the SKULL full moment tensor published in Dreger & Woods (2002). SKULL was a tectonic earthquake, which we would expect to be mainly double-couple. We do find that the mechanism is dominated by a double-couple component, and thus there is little difference between the deviatoric mechanism and the results from the Method 1 and Method 2 full moment tensor inversions (Fig. 5, Tables 2 and 5). We find similar results for the other two tectonic earthquakes, LVTEC and MIYTEC, as well as LV5 and LV6. While LV5 and LV6 are members of the 1997 Long Valley earthquake swarm, these earthquakes appear to not be directly related to volcanic processes, although the earthquakes could have occurred on pre-existing faults after being trigged by stress transfer from seismic activity and deformation in the resurgent dome.

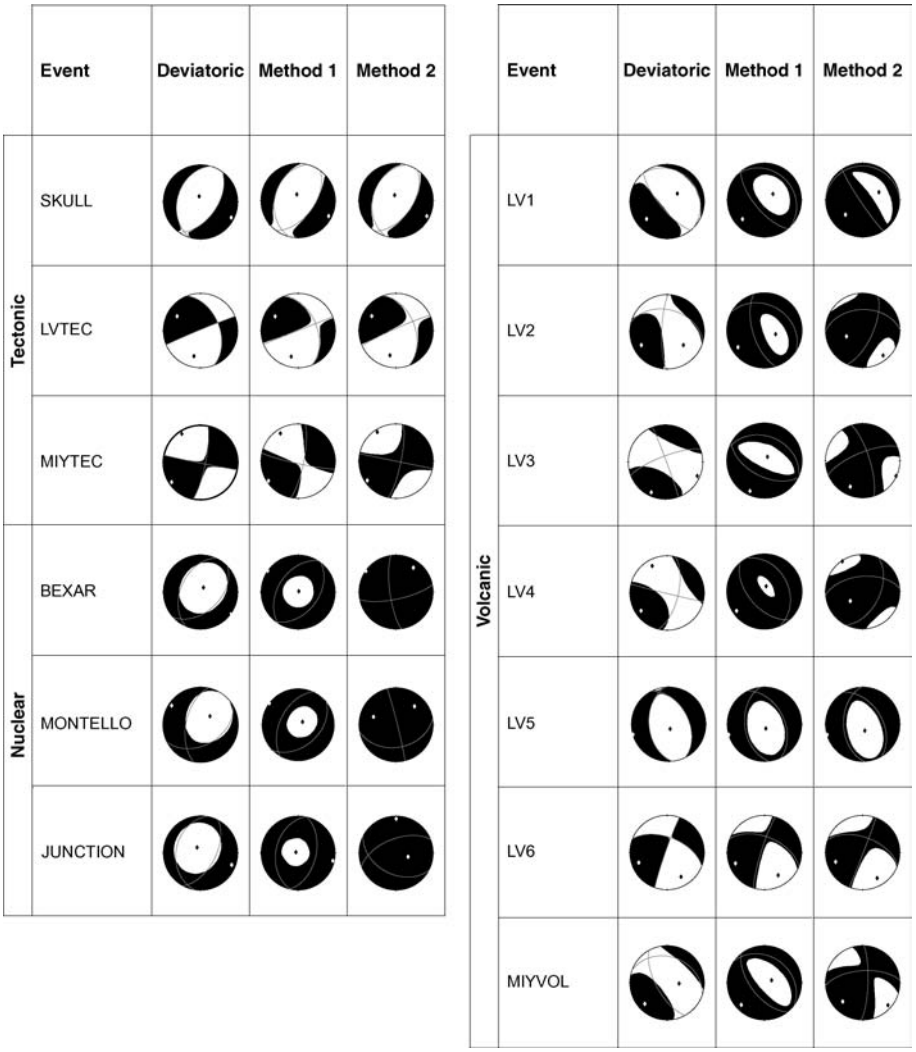

Figure 5. Comparison of deviatoric moment tensors inversions, full moment tensor inversions computed using the flawed methodology (Method 1) and full moment tensor inversions computed using the corrected methodology (Method 2). The nodal planes of the double-couple component are plotted with grey lines. Diamonds indicate the orientation of the pressure and tension axes. Method 2 produces mechanisms for the three nuclear explosions (BEXAR, JUNCTION and MONTELLO), which are substantially more explosive in character than the old mechanisms. These new mechanisms also have smaller M_W.

Table 5. Moment, moment magnitude and epsilon values for full moment tensor inversions.

		Deviatoric			Method 1			Method 2		
Event	M_L	Moment	M_w	ε	Moment	M_w	ε	Moment	M_w	ε
SKULL	6.2	306.30	5.66	0.016	288.60	5.64	0.054	311.30	5.66	0.003
BEXAR	5.6	3.96	4.40	0.278	9.32	4.65	0.373	5.46	4.49	0.106
MONTELLO	5.4	6.19	4.53	0.266	12.16	4.72	0.299	7.85	4.60	0.262
JUNCTION	5.5	3.29	4.35	0.370	9.89	4.66	0.441	6.51	4.54	0.423
LVTEC	—	98.75	5.33	0.002	99.04	5.33	0.012	99.46	5.33	0.024
LV1	—	8.76	4.63	0.117	10.85	4.69	0.019	9.01	4.64	0.376
LV2	—	20.61	4.88	0.205	29.91	4.98	0.243	29.83	4.98	0.002
LV3	—	6.31	4.53	0.437	9.12	4.64	0.311	7.57	4.59	0.107
LV4	—	19.78	4.86	0.336	32.86	5.01	0.296	31.96	5.00	0.161
LV5	—	28.90	4.97	0.010	31.48	5.00	0.049	25.89	4.94	0.072
LV6	—	11.70	4.71	0.005	12.01	4.72	0.067	11.88	4.72	0.051
MIYTEC	—	4395	6.43	0.027	4636	6.44	0.175	4573	6.44	0.093
MIYVOL	—	1814.	6.17	0.377	2200	6.23	0.247	1825	6.17	0.310

Note: Moments are given in 10^{15} N m and are calculated using the methodology of Silver & Jordan (1982).
$\varepsilon = \left|m_3^*/m_1^*\right|$ where m_i^* are the deviatoric eigenvalues of the moment tensor and $\left|m_1^*\right| \geq \left|m_2^*\right| \geq \left|m_3^*\right|$ (Dziewonski *et al.* 1981).

Our inversions of the NTS explosions (BEXAR, MONTELLO and JUNCTION) have very large isotropic components. The small deviatoric part of these mechanisms seems to be due to two different mechanisms. For events BEXAR and MONTELLO, the deviatoric component appears to be tectonic release on either north–south right-lateral or east–west left-lateral faults. In this case, the northeast striking tension axis is consistent with inferred stress and focal mechanisms of natural earthquakes occurring in the Basin and Range province. For the JUNCTION explosion, the deviatoric part is a mixture of a vertically oriented CLVD and a reverse fault. This is consistent with a mechanism of dynamically driven block faulting over a buried source as suggested by Masse (1981).

Unlike the findings from some previous studies of nuclear explosions, the source mechanisms for the NTS events presented in this study truly look like explosions. However, as Dreger & Woods (2002) note, these NTS explosions were ideally located since they were at regional distances from large seismic networks and had well-studied travel paths. Moment tensor inversions of nuclear explosions in regions with poorly understood travel paths and low quality or scarce data may not be able to resolve the isotropic part of the source mechanism without additional waveform modelling and path calibration. Regardless of its value for nuclear monitoring, the inversion scheme presented in this paper results in improved full moment tensor inversions, and this, in turn, will lead to a better understanding of complex source mechanisms.

ACKNOWLEDGMENTS

We used data from broad-band stations in the TERRAscope network and the Berkeley Digital Seismic Network for events located in California and Nevada and data from the F-net Broadband Seismograph Network for the Miyakejima earthquake. Hiroo Kanamori and Sean Ford helped improve the manuscript. Contribution number 9163 of the Caltech Seismological Laboratory.

REFERENCES

Dreger, D. & Woods, B., 2002. Regional distance seismic moment tensors of nuclear explosions, *Tectonophysics,* **356,** 139–156.

Dreger, D.S., Tkalcic, H. & Johnston, M., 2000. Dilational processes accompanying earthquakes in the Long Valley Caldera, *Science,* **288,** 122–125.

Dufumier, H. & Rivera, L., 1997. On the resolution of the isotropic component in moment tensor inversion, **131,** 595–606.

Dziewonski, A.M., Chou, T.-A. & Woodhouse, J.H., 1981. Determination of earthquake source parameters from waveform data for studies of global regional seismicity, *J. geophys. Res.,* **86,** 2825–2852.

Ford, S.R., Dreger, D.S. & Walter, W.R., 2007. Identifying isotropic events using an improved regional moment tensor inversion technique, in *Proceedings of the 29th Monitoring Research Review: Ground-Based Nuclear Explosion Monitoring Technologies*, National Nuclear Security Administration LA-UR-07-5613.

Fukuyama, E. & Dreger, D.S., 2000. Performance test of an automated moment tensor determination system for the future "Tokai" earthquake, *Earth Planets Space,* **52,** 383–392.

Furuya, M., Okubo, S., Miyajima, R., Meilano, I., Sun, W., Tanaka, Y. & Miyazaki, T., 2003. Mass budget of the magma flow in the 2000 volcano-seismic activity at the Izu-islands, Japan, *Earth Planets Space,* **55,** 375–385.

Helmberger, D.V., 1983. Theory and application of synthetic seismograms, in *Earthquakes: Observation, Theory and Interpretation*, pp. 174–222, eds Kanamori, H. & Boschi, E., North-Holland, Amsterdam.

Herrmann, R.B. & Hutchensen, K., 1993. Quantification of m_{Lg} for small explosions, in *Report PL-TR-93-2070*, 90 pp., Phillips Laboratory, Hanscom Air Force Base, MA.

Jost, M.L. & Herrmann, R.B., 1989. A student's guide to and review of moment tensors, *Seism. Res. Lett.,* **60**(2), 37–57.

Julian, B.R. & Sipkin, S.A., 1985. Earthquake processes in the Long Valley Caldera area, California, *J. geophys. Res.,* **90**(13B), 11 155–11 169.

Knopoff, L. & Randall, M.J., 1970. The compensated linear-vector dipole: a possible mechanism for deep earthquakes, *J. geophys. Res.,* **75**(26), 4957–4963.

Langston, C.A., 1981. Source inversion of seismic waveforms: the Koyna, India, earthquakes of 13 September 1967, *Bull. seism. Soc. Am.,* **71**(1), 1–24.

Masse, R.P., 1981, Review of seismic source models for underground nuclear explosions, *Bull. seism. Soc. Am.,* **71**(4), 1247–1266.

Nishimura, T., Ozawa, S., Murakami, M., Sagiya, T., Tada, T., Kaidzu, M. & Ukawa, M., 2001. Crustal deformation caused by magma migration in the northern Izu Islands, Japan, *Geophys. Res. Lett.,* **28**(19), 3745–3748.

Pasyanos, M.E., Dreger, D.S. & Romanowicz, B., 1996. Toward real-time estimation of regional moment tensors, *Bull. seism. Soc. Am.,* **86**(5), 1255–1269.

Patton, H.J., 1988. Source models of the HARZER explosion from regional observations of fundamental-mode and higher mode surface waves, *Bull. seism. Soc. Am.,* **78**(3), 1133–1157.

Saikia, C.K., 1994. Modified frequency-wavenumber algorithm for regional seismograms using Filon's quadrature: modelling Lg waves in eastern North America, *Geophys. J. Int.,* **118,** 142–158.

Silver, P.G. & Jordan, T.H., 1982. Optimal estimation of scalar seismic moment, *Geophys. J. R. astr. Soc.,* **70,** 755–787.

Templeton, D.C. & Dreger, D.S., 2006. Non-double-couple earthquakes in the Long Valley volcanic region, *Bull. seism. Soc. Am.,* **96**(1), 69–79, doi:10.1785/0120040206.

Woods, B.B., Kedar, S. & Helmberger, D.V., 1993. M_L:M_0 as a regional seismic discriminant, *Bull. seism. Soc. Am.,* **83**(4), 1167–1183.